PERGAMON

Solid-State Electronics 45 (2001) 703–709

SOLID-STATE ELECTRONICS

A general-purpose software for optical characterization of thin films: specific features for microelectronic applications

S. Bosch *, J. Ferré-Borrull, J. Sancho-Parramon

Departament de Física Aplicada i Optica, Universitat de Barcelona, Diagonal 647, 08028 Barcelona, Spain

Received 9 February 2000; received in revised form 1 February 2001

Abstract

We present a detailed description of the features and capabilities of a new software for the optical characterization of thin films from spectrophotometric and/or ellipsometric measurements. The program allows the analysis of a wide range of multi-layered structures, either with respect to the composition, microstructure or thickness of any of the layers. Several spectra corresponding to different measurement techniques of a single sample may be fitted simultaneously. A short description of the dispersion models actually implemented to represent the materials is given. Several examples of use are discussed. These have been selected to illustrate important aspects that may be relevant to microelectronic applications. © 2001 Elsevier Science Ltd. All rights reserved.

Keywords: Optical characterization of materials; Thin films

1. Introduction

Computer aided optical characterization is a well-established field for analyzing thin film stacks [1,2]. Many commercial software packages are available for this purpose [3] so that most of the issues arising in thin film technology daily work can be successfully addressed. However, this is not usually the case when new research topics are undertaken since, typically, the problem has not been addressed and specific software developments (not implemented in the available packages) are needed. We present a PC program which has been designed as a versatile tool for interpreting ellipsometric and/or spectrophotometric measurements, including some very specific features, such as:

- the simultaneous fitting of various spectra obtained from one single sample,
- the implementation of effective medium computations for more than two materials,
- the estimation of the confidence limits for any of the parameters determined by the computation program.

Our group has developed these specific features in the recent years in the frame of several research topics. Below, when describing our software, we will summarize the main ideas involved and will provide the corresponding references.

The optical properties of a multi-layered structure (Fig. 1) formed by different materials are usually completely defined by the thickness of the slabs and a set of parameters for each layer (according to the model that may be applied to it). Our program is designed to allow inferring from experimental measurements any of the parameters (including the thicknesses) which define the stack. This is a very general approach, not restricted in the number or type of unknowns involved.

In our scheme, as illustrated in Fig. 1, a 'layer' in the computation program may be:

- any homogeneous slab of deposited material,
- any layer consisting of a mixture of two or more deposited materials,

* Corresponding author. Tel.: +34-93-402-1203; fax: +34-93-402-1142.

E-mail address: sbp@optica.fao.ub.es (S. Bosch).

0038-1101/01/$ - see front matter
PII: S0038-1101(01)00092-2

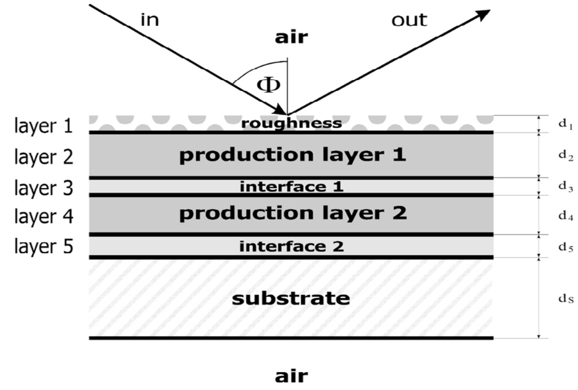

Fig. 1. Sketch of a multi-layered sample.

- any interface between deposited layers,
- a thin slab representing the roughness of the outermost surface.

The first two possibilities correspond to "production" layers, this is, layers intentionally manufactured. On the other hand, the two last possibilities correspond to "subsequent" layers, which appear later on (intentionally or not) in the stack because of interdiffusion of material between layers, the roughness in the substrate or layers, etc.

In our computation procedures the contribution of the two sides of the substrate can be taken into account by considering that the light beams reflected at the two faces are added on an intensity (incoherent) basis, rather than on an amplitude (coherent) superposition, as required for the layers. Moreover, the substrate can be considered semi-infinite as well, this is, without including the backside reflections. This is adequate for the cases where the backside of the substrate is grinded, as customary in ellipsometry, or when substrates are highly absorbing. The computations allow any incidence angle and, in case of spectrophotometric data, these can correspond to p, s or 'natural' polarization.

2. Modeling the layers: detailed description

Our goal is the precise optical characterization of a layered structure for a certain wavelength (or photon energy) range. We have already mentioned that the very definition of the structure is usually not straightforward, since not only the layers intentionally produced are present but also other layered interfaces may exist. As mentioned, some of the possibilities are: interdiffusion of materials, roughness, porosity... It is the task of the physicist or engineer to elucidate what is the right structure to be proposed to accurately represent the samples under analysis. For the "production" layers, there are many models to describe its optical behavior, depending mainly on the type of material (dielectric, metal or semiconductor) and spectral range considered. On the other hand, in the case of the "subsequent" layers it is customary to model them within the sample by means of effective medium approximation (EMA) theories (see below for a short description). From the point of view of computations, a model is, simply, a dispersion formula for n and k, the real and imaginary part of the complex refractive index of the material. We now briefly outline the models implemented in our program, with a more detailed description of our recent contributions.

2.1. Cauchy model (with exponential absorption)

It is useful for dielectric materials, far from the absorption bands [4]. The formulae are:

$$n(\lambda) = n_0 + \frac{n_1}{\lambda^2} + \frac{n_2}{\lambda^4}, \qquad k(\lambda) = k_0 \exp\left(\frac{k_1}{\lambda}\right). \tag{1}$$

Note that this model is defined by five parameters n_0, n_1, n_2, k_0 and k_1.

2.2. Sellmeier model

It is very similar to the previous one. The formulae are:

$$n(\lambda) = \sqrt{1 + \frac{A_1\lambda^2}{\lambda^2 - A_2}}, \qquad k(\lambda) = 0, \tag{2}$$

that include only two parameters A_1 and A_2.

2.3. Lorentz oscillator

This is the most fundamental description of a dielectric material within the electromagnetic theory [4]. The refractive indices are (in terms of the wavenumber σ):

$$n(\sigma) = \left[\tfrac{1}{2}\left(\sqrt{\varepsilon'^2 + \varepsilon''^2} + \varepsilon'\right)\right]^{1/2},$$
$$k(\sigma) = \left[\tfrac{1}{2}\left(\sqrt{\varepsilon'^2 + \varepsilon''^2} - \varepsilon'\right)\right]^{1/2}, \tag{3a}$$

$$\varepsilon'' = 2nk, \quad \varepsilon' = n^2 - k^2, \quad \varepsilon = \varepsilon' + \mathrm{i}\varepsilon'';$$
$$\varepsilon' = \varepsilon_\infty + \frac{F(\sigma_0^2 - \sigma^2)}{(\sigma_0^2 - \sigma^2)^2 + (\Gamma\sigma)^2}, \quad \Gamma = \frac{\gamma}{2\pi c}, \tag{3b}$$
$$\varepsilon'' = \frac{F(\Gamma\sigma)}{(\sigma_0^2 - \sigma^2)^2 + (\Gamma\sigma)^2}, \quad F = (\varepsilon_0 - \varepsilon_\infty)\sigma_0^2.$$

Several oscillators can be simultaneously considered. The required parameters are ε_∞ plus three quantities (F, Γ, σ_0) for each oscillator.

2.4. Tauc–Lorentz expressions

This dispersion model has been successfully used for amorphous semiconductors and insulators [5] and is a generalization of previous theoretical approaches like the Tauc model [6] and the Forouhi–Bloomer parametrization [7]. It is, in fact, a modification of the Lorentz oscillator just presented above and a practical comparison between these models has been recently presented for amorphous carbon films [8]. The mathematical expressions involved are really cumbersome [5] and will not be presented here explicitly.

2.5. Bruggeman effective medium approximation

In the case of layers that can be considered a mixture of materials, the electromagnetic description can be done in terms of an EMA [9]. As a consequence, besides the representation of actual mixtures of components, in the framework of our computation approach, the EMA will enable us to model interfacial layers (i.e., zones where one can assume to have a mixture of the materials from two consecutively deposited layers) as well as roughness (where air is mixed with the material of the top layer). Historically, the first EMA theory was developed by Bruggeman [10]. The resulting optical constants will depend mainly on the volume fraction of the components (*host* material and *inclusions*). Nevertheless, the geometrical configuration of the mixture (shape or type of inclusions within a host material) is also relevant and may be introduced in a generalised EMA theory by including a screening parameter y [11]. If we name ε_i the dielectric constants of the components, f_i their volume fractions and y the screening parameter, the mathematical expression for the effective dielectric constant ε in terms of the ε_i, f_i and y is given (in implicit form) by

$$0 = \sum_i f_i \frac{\varepsilon_i - \varepsilon}{\varepsilon_i + y\varepsilon}. \quad (4)$$

2.6. Lorentz–Lorenz effective medium approximation

This approximation differs from the Bruggeman theory in the consideration of what is the *host* material and what are the *inclusions*. Now the effective dielectric constant is given by

$$\frac{\varepsilon - 1}{\varepsilon - y} = \sum_i f_i \frac{\varepsilon_i - 1}{\varepsilon_i + y}. \quad (5)$$

Major computational problems arise when more than two materials are present in a mixture, since (in the spectroscopic case) Eqs. (4) and (5) have to be solved for each wavelength starting from the spectral data of the individual components, with only an approximate knowledge of their volume fractions. A convenient numerical procedure to deal with the last two equations has been recently developed in Ref. [12]. It is important to note that the methods presented in this reference provide a suitable computational framework for all the practical situations that can be modeled through EMA theories involving more than two constitutive materials, like considering a superficial roughness (represented as a void fraction) on a two-material mixture layer, for example.

3. Computational scheme

According to the modeling of the layers just exposed, finally each layer can be fully described by its geometrical thickness and a set of variable number of parameters, according to the complexity of the model we are considering for it. The complete stack (including the substrate) is defined by the full set of model parameters and thicknesses. In practical situations, some of these values will be known (for example the optical constants of the substrate), while others are only approximately estimated and will be the unknowns of our characterization process.

There is one main difference between a numerical procedure developed for a specific problem and a general-purpose software: in this second case the computational scheme must be broad enough to cover all the conceivable cases. We have been involved in recent years in a series of investigations about monochromatic ellipsometry [13–16], spectroscopic ellipsometry [17–19] and spectrophotometry [20–22], providing (in all the cases) some specific new ideas which have been the basis for the work we are presenting now.

Our computational approach is as follows. Assume, first, that our data consist of a single set of n measurements y_i, $i = 1, \ldots, n$, corresponding to the independent variables x_i (say, for example, an spectrum of reflectance values y_i at normal incidence for wavelengths x_i). Once all the defining parameters (say m quantities in total: p_1, $p_2, \ldots, p_m$) take a value and assuming that we have an estimation of the error σ_i associated to each single data y_i, standard thin film computation procedures [2] allow us to compute the chi-square function

$$\chi^2(p_1, p_2, \ldots, p_m) = \frac{1}{n - m - 1} \times \sum_{i=1}^{n} \left(\frac{y_i - y(x_i; p_1, p_2, \ldots, p_m)}{\sigma_i} \right)^2. \quad (6)$$

This will be the merit function in a minimization procedure in the space of the unknown parameters. We still have to choose the minimization algorithm: we use the 'Downhill Simplex' method [23] because is very easy to adapt to our situation where the number of unknowns and the range of their increments are quite variable. Moreover, the explicit dependence between χ^2 and the parameters is usually very complex, so that other algorithms (such as those requiring the computation of derivatives) are inappropriate. The optimization is started from the point in the parameter space defined by the estimated values (guess) of the unknown parameters.

Once the optimization is done our numerical procedures also include the computation of the correlated and uncorrelated confidence limits for the calculated parameters. These tasks require knowing the *curvature matrix* (second partial derivatives of χ^2) at the end point of the optimization process. The determination of confidence limits for the parameters is a necessary step for a complete interpretation of the results from a physical point of view [23].

One very specific feature of our approach is the ability to perform the minimization of a χ^2 that takes into account simultaneously up to 10 spectrophotometric and/or ellipsometric spectra. This fact may be accomplished by including in the sum (6) the terms corresponding to all the spectra, affected by their respective error estimations σ_i. It is worth noting that this important feature is only possible by using the χ^2 estimator as the merit function to minimize, since each term in the sum (6) is a dimensionless number that allows mixing any kind of measured data into a single merit function. Moreover, it is clear that trying to refine a fitting whose value for χ^2 is already around one has no physical significance.

To test and show some of the non-standard capabilities of the program, we have performed two types of computation examples: fitting procedures with simulated data (i.e., computed for an ideal theoretical sample with perfectly known characteristics) and fittings for real spectrophotometric data. Besides, the examples have been chosen to illustrate situations of potential interest in microelectronics.

4. Examples for theoretical samples

4.1. Nanocrystalline silicon in a SiO_2 matrix

Assume an ideal sample consisting of a mixture of SiO_2 (host material, 75% volume fraction) and spherical inclusions of nc-Si (25%) on a silicon substrate (see Fig. 2). Let us take for the thickness of the layer $d = 400$ nm. Let us consider that the layer can be modeled by the Bruggeman EMA formula (4), where the optical constants of the two component materials (SiO_2 and nc-Si) are known [24]. Within this framework, the ellipsometric spectra ($\sin(\Delta)$, $\cos(2\psi)$) in the range 300–900 nm have been computed, supposing an incidence angle of 60°. Fig. 3 plots the ψ-part as a continuous line. We have supposed that there is no contribution from light re-

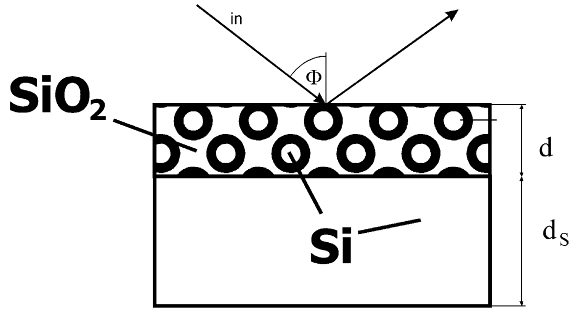

Fig. 2. Nanocrystalline silicon inclusions in SiO_2.

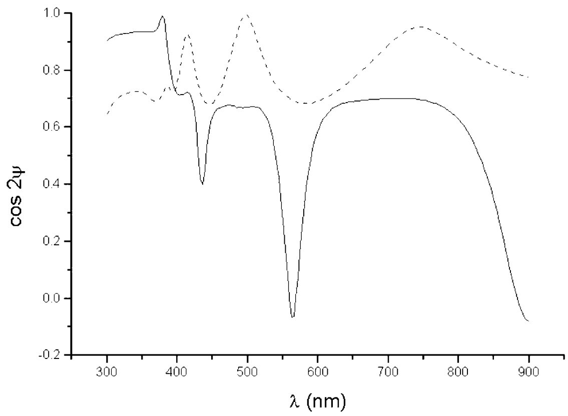

Fig. 3. Simulated ellipsometric ψ-data for the ideal sample sketched in Fig. 2 (solid line: $d = 400$ nm, volume fraction of the Si inclusions = 25%) and for the initial guess (dashed line: $d = 250$ nm, volume fraction of the Si inclusions = 45%).

flected in the back-surface of the substrate, as usual in ellipsometry.

Following the same EMA model above, we will consider that our unknown parameters are the thickness d and the volume fractions of the components. If our guesses are $d = 250$ nm and 45% volume fraction of nc-Si, the computed ψ-data for the corresponding stack is the dashed line of Fig. 3.

To illustrate the working capabilities of our program, we have simulated a practical situation where our experimental data are, in fact, computed. Taking the continuous line of Fig. 3 as the measured spectrum and starting the minimization process from the guess just mentioned, the algorithm is able to recover the actual values for d and the volume fractions corresponding to the continuous line, despite of the large initial difference between the spectra.

4.2. Porous silicon or nanocrystalline silicon layers

We now consider another ideal sample consisting of a layer formed by packed small spheres of nc-Si, leaving a

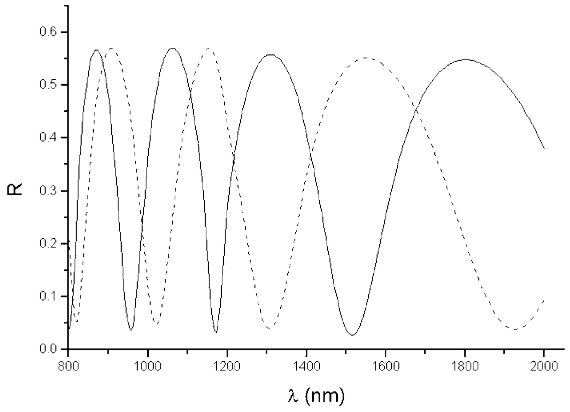

Fig. 4. Simulated reflectance data for our second ideal layer (solid line: $d = 700$ nm, volume fraction of voids = 10%) and for the initial guess (dashed line: $d = 650$ nm, volume fraction of voids = 20%).

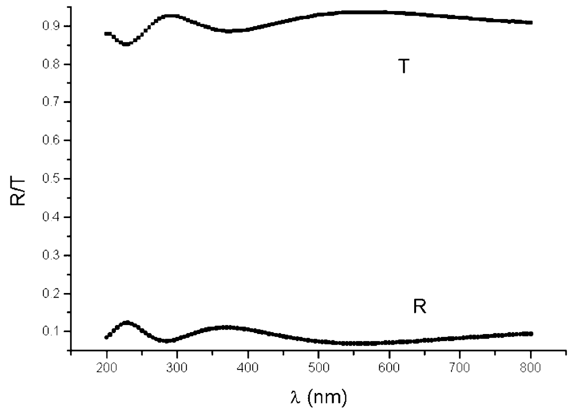

Fig. 5. Reflectance and transmittance spectra of our quartz sample.

10% volume fraction of voids between the granules. The substrate is quartz (semi-infinite, i.e. without back-surface reflection) and the thickness of the layer is taken as $d = 700$ nm. The configuration is conceptually similar to that of Fig. 2, simply replacing the SiO_2 by voids (i.e., air having unity refractive index), making up the 10% volume fraction of the layer. Assuming again that the layer can be modeled by an EMA approximation, the reflectance spectrum of this ideal sample, computed at 20° incidence angle, is shown in Fig. 4 as a continuous line.

Again, we will use the same EMA modeling, where our unknown parameters are the thickness d and the volume fraction of voids (or of the nc-Si spheres, since they are values complementary to 100%). Taking initially (as a guess or approximate values) $d = 650$ nm and 20% fraction of voids, the computed spectrum is shown as the dashed line of Fig. 4.

As in the previous example, starting our minimization procedure from these initial values, the algorithm recovers the right values of thickness and volume fraction ($d = 700$ nm and 10% voids, assumed for the continuous line spectrum of our ideal sample).

5. Characterization of a layer over a very thin interfacial layer

The software we have presented has a wide range of applications in the characterization of thin films. We have chosen now an example form the field of coatings for UV laser optics, consisting of the characterization of a LaF_3 layer deposited over an interfacial layer. Two samples were obtained from the same batch process (thus, having LaF_3 layers of equal thickness), one on quartz and the other on CaF_2. To improve adhesion on quartz, this substrate was previously coated with a very thin layer of MgF_2 (about 10 nm thick) and this fact has to be included in the characterization process. We have used our software for the characterization of the two samples. For each substrate we will fit simultaneously the experimental data corresponding to reflectance and transmittance spectra at normal incidence in the range 200–800 nm. Fig. 5 plots these two spectra for the quartz sample. Note that the reflectance corresponds to a double sided substrate (i.e., backsurface reflection is included) with light incident on the film side. The accuracy in the measurement was evaluated to be 0.15% for transmittance and 0.30% for reflectance, in the whole range. These values correspond to all σ_i in our expression (6) and, accordingly, give four times weight in the merit function to the transmittance data than to the reflectance ones.

It is instructive to illustrate the complete characterization process as it was performed and not only the final results, since there are interesting aspects to be commented. First, we know from the simple observation of the transmittance curve, that all the materials involved are basically transparent in the spectral region of interest, although some absorption becomes evident at short wavelengths. Besides, the optical constants of the substrates are well defined a priori in the present case [24]. Accordingly, a Cauchy model (1) should be adequate and will be used here.

It is known that reflectance measurements are less affected by absorption than transmittance ones. Thus, it is convenient to begin from the reflectance curve, neglecting the existence of the interface layer and, consequently, by fitting the curve from the most basic three remaining parameters: the thickness and the coefficients n_0 and n_1 of the LaF_3 layer. The results of this minimization for the quartz sample is: $n_0 = 1.599$, $n_1 = 3997$ nm^2 and thickness 171.6 nm ($\chi^2 = 0.28$). The

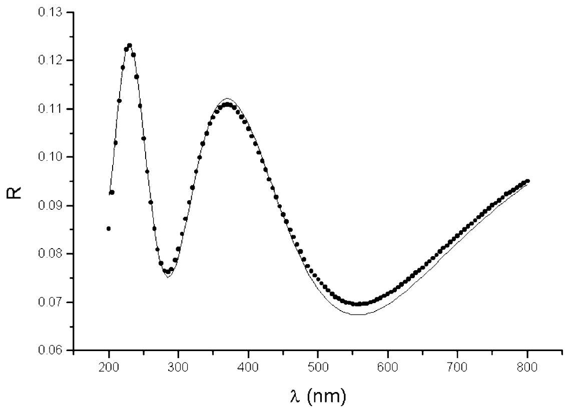

Fig. 6. Initial fitting of the reflectance spectrum of the quartz sample (the dots are the data).

plot of the corresponding reflectance, compared to the measured data is presented in Fig. 6. Next, if we analyze how well these values fit the experimental transmittance, we easily conclude that some absorption has to be introduced in the LaF_3 layer, since the fitting for the transmittance is not good. The simultaneous fitting of the R and T data, taking thickness, n_0, n_1, k_0 and k_1 as variables, leads us to the following results: $n_0 = 1.582$, $n_1 = 5075$ nm^2, $k_0 = 1.35 \times 10^{-5}$, $k_1 = 1175$ nm, and thickness 171.8 nm ($\chi^2 = 0.93$). Fig. 7 illustrates the quality of the adjustment. Next, we can easily check that no significant improvement is obtained by introducing a new term n_2 in Eq. (1), and we simply take $n_2 = 0$. Performing the same calculations for the CaF_2 substrate, the results were: $n_0 = 1.599$, $n_1 = 4431$ nm^2, $k_0 = 1.6 \times 10^{-5}$, $k_1 = 1143$ nm, and thickness 175.4 nm ($\chi^2 = 0.56$). The complete series of results is summarized in Tables 1 and 2.

So far we have not considered the interfacial layer that we know it was indeed deposited on the quartz substrate prior to the manufacture of the main layer. Since we know the interfacial layer is very thin, our

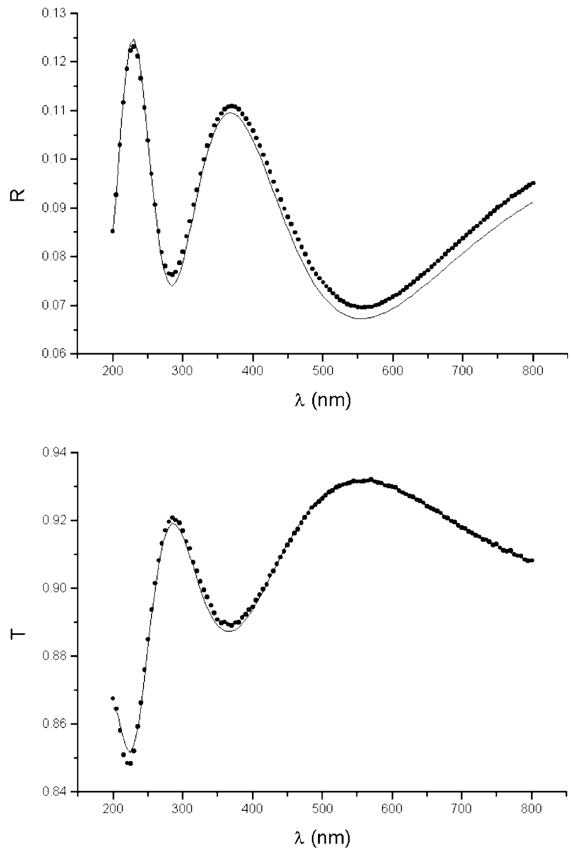

Fig. 7. Simultaneous fitting of R and T for the quartz sample (the dots are the data).

procedure has been safe to avoid the simultaneous minimization of many parameters. It is now the right moment to introduce the interface in our model, by using the results just presented for the characterization of the LaF_3 layer on quartz, but also including in the minimization routine an adjustable thickness for a MgF_2 layer of known refractive index [24]. The results ob-

Table 1
Results of the successive steps in the fitting of the R and T data for the quartz substrate

	Thick (nm)	n_0	n_1 (nm^2)	k_0	k_1 (nm)	χ^2
R	171.6	1.599	3997			0.28
$R+T$	171.8	1.582	5075	1.35×10^{-5}	1175	0.93
$R+T+$ interf	175.7	1.585	4344	1.01×10^{-5}	1228	0.62

Table 2
Results of the successive steps in the fitting of the R and T data for the CaF_2 substrate

	Thick (nm)	n_0	n_1 (nm^2)	k_0	k_1 (nm)	χ^2
R	175.3	1.598	3962			0.34
$R+T$	175.4	1.589	4431	1.60×10^{-5}	1143	0.56

tained are as follows. For the LaF_3 layer: $n_0 = 1.585$, $n_1 = 4344$ nm^2, $k_0 = 1.01 \times 10^{-5}$, $k_1 = 1228$ nm, and thickness 175.7 nm (last row of Table 1). For the MgF_2 interface layer the thickness obtained was 9.4 nm. The merit function for this fitting was $\chi^2 = 0.62$. Thus, the comparison of the results for the quartz and the CaF_2 substrates evidences the existence of the interfacial MgF_2 layer on quartz: the thicknesses of the two LaF_3 layers are now much more similar (175.4 nm on CaF_2 and 175.7 nm on quartz, whereas assuming no interface this last value was 171.8 nm) and the final merit function has also significantly decreased from 0.93 to 0.62. Note that the versatility of our software and the suitable definition of the merit function has evidenced a very thin interface (about 10 nm) whose refractive index is quite similar to that of the substrate.

6. Conclusions

The accurate and versatile optical modeling of multilayers is essential for many research and development tasks in optics and electronics. While most of the standard tasks in thin film technology may adequately be addressed by means of any of the excellent software packages commercially available, the innovative research topics usually require a open software where one may easily introduce either modifications or new theoretical models. We have presented a software tool for the analysis of spectrophotometric and ellipsometric spectra that is very general, allows to model interfacial and roughness layers (where there is a mixture between the upper and the lower materials) by means of EMA computations for more than two materials and is able to determine any of the parameters which define the stack (not restricted in the number or type of unknowns involved) with their corresponding confidence limits.

We have illustrated the computation procedures with two types of examples. First, we have fitted simulated data (previously computed by assuming a precisely defined theoretical sample), showing the capabilities of the software for mixtures of materials with a poor estimation of the actual volume fractions. Second, we have presented a worked real case where a LaF_3 layer is characterized and, simultaneously, a very thin interface layer (with a refractive index quite similar to the substrate one) is evidenced.

Acknowledgements

The authors gratefully acknowledge the support of the European Commission (TMR-network UV-coatings, contract-no. ERBFMRX-CT97-0101) and thank E. Quesnel for providing experimental data.

References

[1] Thelen A. Design of optical interference coatings. New York: Macmillan; 1987.
[2] Berning PH. Physics of thin films. vol. 1, New York: Academic Press; 1963. p. 69–121.
[3] Dobrowolski JA. Optics Photon News 1997. p. 25–33.
[4] Born M, Wolf E. Principles of optics. Oxford: Pergamon Press; 1975.
[5] Jellison Jr GE, Modine FA. Appl Phys Lett 1996;69:371–3.
[6] Tauc J, Grigorovici R, Vancu A. Phys Status Solidi 1996;15:627.
[7] Forouhi AR, Bloomer I. Phys Rev B 1986;34:7018.
[8] Canillas A, Polo MC, Andújar JL, Sancho J, Bosch S, Robertson J, Milne WI. Spectroscopic ellipsometric study of tetrahedral amorphous carbon films: optical properties and modelling. Diamond Relat Mater, in press.
[9] Berthier S. Optique des milieux composites. Polytechnica, Paris, 1993.
[10] Bruggeman DAG. Ann Phys (Leipzig) 2000;453:9–17.
[11] Aspnes DE, Theeten JB, Hottier F. Phys Rev B 1979;20:3292–302.
[12] Bosch S, Ferré-Borrull J, Leinfellner N, Canillas A. Effective dielectric function of mixtures of three or more materials: a numerical procedure for computations. Surf Sci, in press.
[13] Bosch S. Surf Sci 1993;289:411–7.
[14] Bosch S, Monzonís F. Surf Sci 1994;321:156–60.
[15] Bosch S, Monzonís F. J Opt Soc Am A 1995;12:1375–9.
[16] Bosch S, Monzonís F. Semicond Sci Technol 1995;10:1634–7.
[17] Bosch S, Monzonís F, Masetti E. Thin Solid Films 1996;289:54–8.
[18] Bosch S, Pérez J, Canillas A. Appl Opt 1998;37:1177–9.
[19] Popov KV, Tikhonravov AV, Campmany J, Bertrán E, Bosch S, Canillas A. Thin Solid Films 1998;313-314:379–83.
[20] Bosch S, Leinfellner N, Quesnel E, Duparré A, Ferré-Borrull J, Guenster S, Ristau D. "Optical characterization of materials deposited by different processes: the LaF_3 in the UV-visible region". Proc SPIE, 2000 vol. 4094:15–22.
[21] Bosch S, Leinfellner N, Quesnel E, Duparré A, Ferré-Borrull J, Guenster S, Ristau D. "New procedure for the optical characterization of high quality thin films". Proc SPIE, 2000 vol. 4099:124–30.
[22] Guenster S, Ristau D, Bosch S. "Spectrophotometric determination of absorption in the DUV/VUV spectral range for MgF_2 and LaF_3 thin films". Proc SPIE, 2000 vol. 4099:299–310.
[23] Press et al., WH. Numerical recipes in C. Second edition, Cambridge: Cambridge University Press; 1992 [Chapters 9 and 10].
[24] Palik ED, editor. Handbook of optical constants of solids. New York: Academic Press; 1991.